Original Article

Evaluation of condylar osseous changes using a wireless detector with proton density–weighted imaging sequences

Xing Ming[1#], Xinge Cheng[1#], Chong Tian[1], Wuchao Li[1], Rongpin Wang[1], Chunqi Qian[2,3], Xianchun Zeng[1]

[1]Department of Radiology, Guizhou Provincial People's Hospital, Key Laboratory of Intelligent Medical Imaging Analysis and Accurate Diagnosis of Guizhou Province, International Exemplary Cooperation Base of Precision Imaging for Diagnosis and Treatment, Guiyang, China; [2]Department of Electrical and Computer Engineering, Michigan State University, East Lansing, MI, USA; [3]Department of Radiology, Michigan State University, East Lansing, MI, USA

Contributions: (I) Conception and design: X Ming, X Zeng; (II) Administrative support: X Zeng, R Wang, C Tian; (III) Provision of study materials or patients: X Ming, X Cheng; (IV) Collection and assembly of data: X Cheng, C Tian, W Li; (V) Data analysis and interpretation: X Ming, R Wang, C Qian; (VI) Manuscript writing: All authors; (VII) Final approval of manuscript: All authors.

[#]These authors contributed equally to this work.

Correspondence to: Xianchun Zeng. Department of Radiology, Guizhou Provincial People's Hospital, 83 Zhongshan East Road, Guiyang 550002, Guizhou, China. Email: zengxianchun04@foxmail.com.

Background: Cone-beam computed tomography (CBCT) is the gold standard for evaluating condylar osseous changes. However, the radiation risk and low soft-tissue resolution of CBCT make it unsuitable for evaluating soft tissue such as the articular disc and lateral pterygoid muscle. This study aimed to qualitatively and quantitatively evaluate the feasibility and advantages of using wireless detectors (WD) with proton density–weighted imaging (PDWI) sequences to image condyle changes in patients with temporomandibular disorders (TMD).

Methods: This study involved 20 patients (male =8, female =12; mean age 31.65 years, SD 12.68 years) with TMD. All participants underwent a closed oblique sagittal PDWI scan with head/neck coupling coiling (HNCC) and wireless detector–HNCC (WD-HNCC) on a 3.0 T magnetic resonance imaging (MRI) scanner. Subsequently, the changes in the condyle bones in the scanned images for the 2 image types were scored subjectively and compared qualitatively. The contrast-to-noise ratio (CNR) of the 2 types of scanned images was compared quantitatively. The comparison of CNR differences between the 2 types of images was performed using the paired *t*-test. The kappa statistic was used to test the consistency of quantitative analyses of MRI images between observers. The subjective scores of condylar osseous changes in the 2 types of images were compared by paired rank-sum test. A P value <0.05 was considered statistically significant.

Results: A total of 40 condyles from 20 patients were scanned. Among them, 8 condyles showed no bone changes, and the other 32 condyles demonstrated condylar osseous changes of varying degrees and nature. These 32 condyles were used in the subsequent analysis. As compared to images acquired by HNCC in the PDWI sequence, the WD-HNCC images more clearly showed mandibular osteophyte, bone cortical erosion, subcortical cystic focus, and bone cortical hyperplasia and thickening. In addition, the WD-HNCC was demonstrated to improve image CNR by 158.9% compared to HNCC (28.17±16.01 *vs.* 10.88±6.53; t=8.63; P=0.001).

Conclusions: WD-HNCC in PDWI sequences is suitable for imaging the condylar bone changes of patients with TMD and significantly improves the image quality.

Keywords: Wireless detector (WD); temporomandibular disorders (TMD); temporomandibular joint (TMJ); magnetic resonance imaging (MRI)

Submitted Apr 28, 2022. Accepted for publication Sep 27, 2022. Published online Oct 27, 2022.
doi: 10.21037/qims-22-424
View this article at: https://dx.doi.org/10.21037/qims-22-424

Introduction

Epidemiological studies from all over the world have confirmed the prevalence of temporomandibular disorders (TMD). Globally, approximately 31% of adults and 11% of adolescents experience TMD (1). Condylar osseous change is one of the most common causes and pathological manifestations of TMD, which is characterized by erosion and wearing of the articular surface cartilage and remodeling of subchondral cartilage due to overload (2). Condylar osseous changes in TMD may be one of the symptoms of systemic diseases or may indicate the irreversibility of the disease. These changes are also one of the causes of TMD disc lesions. Medical imaging is of great value in the diagnosis and differential diagnoses of condylar osseous changes.

Research Diagnostic Criteria for Temporomandibular Disorders has recommended cone-beam computed tomography (CBCT) as the modality of choice to evaluate temporomandibular joint (TMJ) osseous changes in both clinical and research settings (3). However, the CBCT radiation is delivered close to the lens and thyroid gland, which are more sensitive to radiation. This increases the risk of radiation in patients with TMD who often need to be examined repeatedly. Therefore, the relatively high radiation dose has limited the use of CBCT for TMD assessment. Currently, magnetic resonance imaging (MRI) is considered the reference method of choice for imaging the soft tissue structures of the TMJ (4-6). However, due to its low sensitivity in condylar bone imaging, MRI provides little or no detectable signal from cortical bone (7).

Recently, animal-based experiments have shown that the resolution and visibility of tiny tissues and organs can be enhanced greatly using a wireless detector (WD). A WD relies on nonlinear capacitance to transfer energy from the externally provided pumping field to weak magnetic resonance (MR) signals. The detector can be implemented as a nonlinear double-frequency resonator, with the lower-resonance mode able to receive MR signals at the Larmor frequency (ω_1) and the higher-resonance mode being sensitive to a pumping field at a frequency (ω_3) that is slightly above $2\omega_1$. The frequency offset between ω_3 and $2\omega_1$ should be at least the imaging bandwidth, so that the "idler signals" created at the difference frequency ($\omega_2 = \omega_3 - \omega_1$) can be filtered out to eliminate destructive interference with MR signals at ω_1. Initially, the WD was used as an implantable detector mounted on the surface of the kidney (8). Subsequently, to image heterogeneous tumors or aorta walls more clearly, the WD was re-engineered with cylindrical symmetry for nonsurgical use inside the digestive tract (9-12). In this study, a disc-shaped WD, which is more suitable for body superficial tissue or organ examination, was used to overcome the sensitivity limitation of conventional MRI in TMJ condylar imaging. This approach utilizes the full advantages of WD in high-resolution imaging of microtissues and organs. This proof-of-concept study aimed to qualitatively and quantitatively evaluate the feasibility and advantages of using WD-coupled head/neck coupling coiling (WD-HNCC) with proton density–weighted imaging (PDWI) sequences to image condylar changes in patients with TMD.

Methods

Participants

The study was conducted in accordance with the Declaration of Helsinki (as revised in 2013). The study was approved by the Institutional Review Board of Guizhou Provincial People's Hospital (No. LYSZ [2019] 186) and informed consent was provided by all individual participants. The study recruited 20 outpatients with TMD who had sought treatment from the Department of Oral and Maxillofacial Surgery at the Guizhou Province People's Hospital in 2020. The participants included 12 females and 8 males, aged between 19 and 58 years old, with a mean age of 31.65 (SD 12.68) years old. The inclusion criteria were as follows: (I) TMD was diagnosed by oral surgeons or oral physicians according to TMD biaxial diagnostic criteria (13); (II) the patient had clinical symptoms such as maxillofacial pain or presence of click or crepitation in joints, mastication difficulty, or mouth-opening limitation in the previous 3 months; and (III) the mandibular condyle of all participants showed at least 1 sign of bone changes such as osteophyte, cortical erosion, subcortical cystic focus, bone thickening, and sclerosis. The exclusion criteria were as follows: (I)

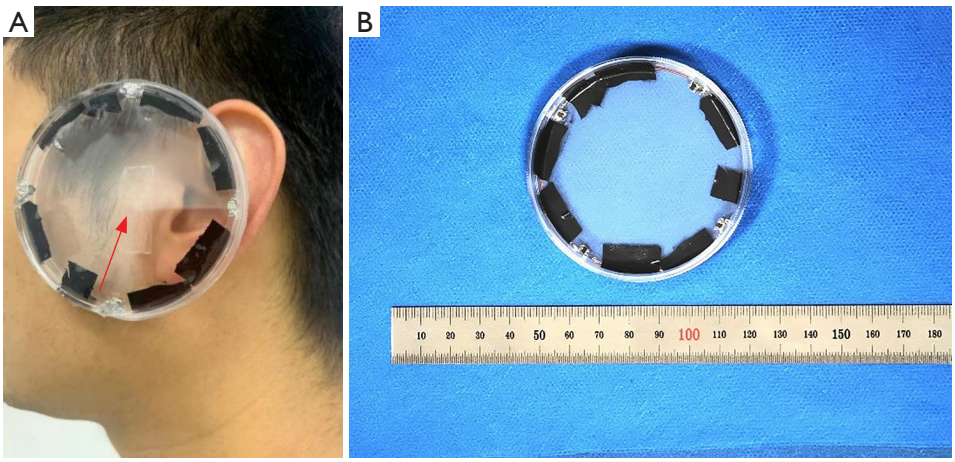

Figure 1 Position of the WD coil (red arrow) which was tightly attached to the surface of the TMJ during MRI scanning (A). Photograph of the WD coil (B). Image A is published with the patient's consent. WD, wireless detector; TMJ temporomandibular joint; MRI, magnetic resonance imaging.

maxillofacial tumor, severe maxillofacial infection, chronic suppurative otitis media, or other maxillofacial diseases; (II) with claustrophobia, fixed dentures, or other MRI contraindications; and (III) an intact condylar osseous structure with poor MRI image quality affecting evaluation.

Imaging equipment and position

MRI data sets were obtained from 20 participants who had been diagnosed with TMD according to the diagnostic criteria for TMD. All participants underwent MRI scanning, and images were produced using a 3.0T MR scanner (Discovery MR 750W; GE Healthcare, Milwaukee, WI, USA) equipped with a 24-channel phased-array coil. The oblique sagittal slices in the fat-suppressed PDWI sequence were scanned at the closed-mouth position with HNCC and WD-HNCC, respectively. The WD coil was fixed to the center of the bilateral TMJ using medical adhesive tape and a sponge (*Figure 1A*), and the scanning range included the entire TMJ region. The scan parameters were as follows: the repetition time/echo time (TR/TE) was set as 2,000/30 ms, the flip angle was 90 degrees, the field of view (FOV) was 150 mm × 150 mm, the matrix was 256×256, the slice thickness was 3 mm, the number of excitations (NEX) was 2 times, and the scanning time was 140 s.

The closed-mouth position refers to the position where the mouth is closed and the posterior teeth are clenched. The positioning line of the oblique sagittal at the closed-mouth position was perpendicular to the long axis of the condylar head.

WD

As shown in *Figure 1B*, the WD has a diameter of 7 cm and can be closely attached to the surface of the TMJ. As compared to the standard HNCC, the WD can observe the lesion area with increased sensitivity, even at a closer distance. While amplifying the local signal in situ, the WD also transmits the enhanced signal to the HNCC by wireless coupling.

Qualitative analysis

All images were analyzed and scored independently by 2 observers, both of whom are senior radiologists, using a double-blind method. All images were viewed on the same monitor under the same conditions. The 2 observers were asked to evaluate the following characteristics for each image (7,14): (I) osteophyte, the marginal bony outgrowths on the condyle; (II) erosion, the irregular surface of condyle, including the collapse or discontinuity of the bone cortex; (III) subcortical cyst, the subcortical circular or fusiform high-signal focus of the condyle in PDWI; and (IV) sclerosis, the extent to which the cortical part of the condylar is thickened and extends to the bone marrow cavity. In addition, a 5-point rating scale [1–5] was used to define the severity of erosion in the condylar head as follows: 1 point was given when the observer was unable to

distinguish between the bone cortex and medullary cavity; 2 points were given when the condylar osseous cortex could be displayed, but the edges and details could not be seen; 3 points were given when the condylar bone cortex was moderately distinguishable, but the edges and details were not clear; 4 points were given when the cortical structure of the condylar bone was displayed completely with good details, but the boundary of condylar osseous changes was not clear; and 5 points were given when the condylar structure and details were displayed completely, and the boundary of condylar osseous changes was clearly shown.

Quantitative analysis

All MRI data images were exported in digital imaging and communications in medicine (DICOM) format and analyzed using ImageJ (National Institutes of Health [NIH], Bethesda, MD, USA). The image intensity profile was plotted along a line crossing the mandibular condyle. The best image for the ramus of the mandible-condyle in the oblique sagittal position was obtained by delineating 2 circular regions of interest (ROIs) with an area of about 5 mm^2 on the subsurface of the condylar joint and the background. In addition, the background noise of each image was measured. The mean signal intensity (SI) and SD values of each group were calculated.

Statistical analysis

The comparison of contrast-to-noise ratio (CNR) differences between the 2 types of images was performed using the paired *t*-test.

In this study, the kappa statistic was used to test the consistency of quantitative analyses of MRI images between observers. The weighted kappa value is between 0 and 1, with a larger value indicating a higher consistency. A kappa value of 0.41–0.60 means moderate consistency; 0.61–0.80, substantial consistency; and 0.81–1, perfect consistency.

The subjective scores of condylar osseous changes in the 2 types of images were compared by paired rank-sum test.

Statistical computations were performed with SPSS 19.0 software (IBM Corp., Armonk, NY, USA). The results with P values of less than 0.05 were considered statistically significant.

Results

A total of 40 condyles were scanned in 20 patients. Among them, there were 8 (20%) condyles with no osseous change (*Figure 2*) and 32 (80%) condyles with differing degrees of change, and the nature of osseous changes were included in the study. The participants consisted of 8 males and 12 females, with an average age of 31.65 (SD 12.68) years. There were 12 (30%) cases of condylar osteophytes (including 4 cases of cortical bone erosion and 2 cases of bone cortical thickening), 6 (15%) cases of cortical and/or subcortical erosion and erosion, 6 (15%) cases of subcortical cystic lesions, and 16 (40%) cases of bone cortical thickening (including 2 cases of cystic lesions).

Qualitative analysis

The image quality of condylar osseous changes scored by the 2 observers showed high consistency, with a value between 0.83 and 0.91. As shown in *Table 1* and *Figures 3-5*, the WD-HNCC images display mandibular osteophyte, bone cortical erosion, subcortical cystic focus, and bone cortical hyperplasia and thickening more clearly as compared to HNCC alone.

Quantitative analysis

When compared with the CNR value obtained via application of HNCC only, the CNR value of WD-HNCC was significantly higher (10.88±6.53 *vs.* 28.17±16.01; t=8.63; P=0.001), as shown in *Figure 6*.

Discussion

The main purpose of this study was to extend the use of WD from animal research to noninvasive imaging of the human TMJ for the first time. The results showed that WD-HNCC improved the image quality of TMD, highlighting condylar osseous changes on the conventional PDWI sequences. Therefore, this study showcases the feasibility of WD-MRI in evaluating condylar osseous changes.

The mandibular condyle is the main component of the TMJ and the only active joint in the maxillofacial region, which is used in important physiological activities such as occlusion and pronunciation. The formation of osteophytes on the surface of the mandibular condyle, the erosion of bone cortex and subcortical cystic foci, and the thickening and sclerosis of bones are pathological manifestations of TMD that indicate its irreversibility (15,16). Therefore, the timely and reliable evaluation of the condyle is of great

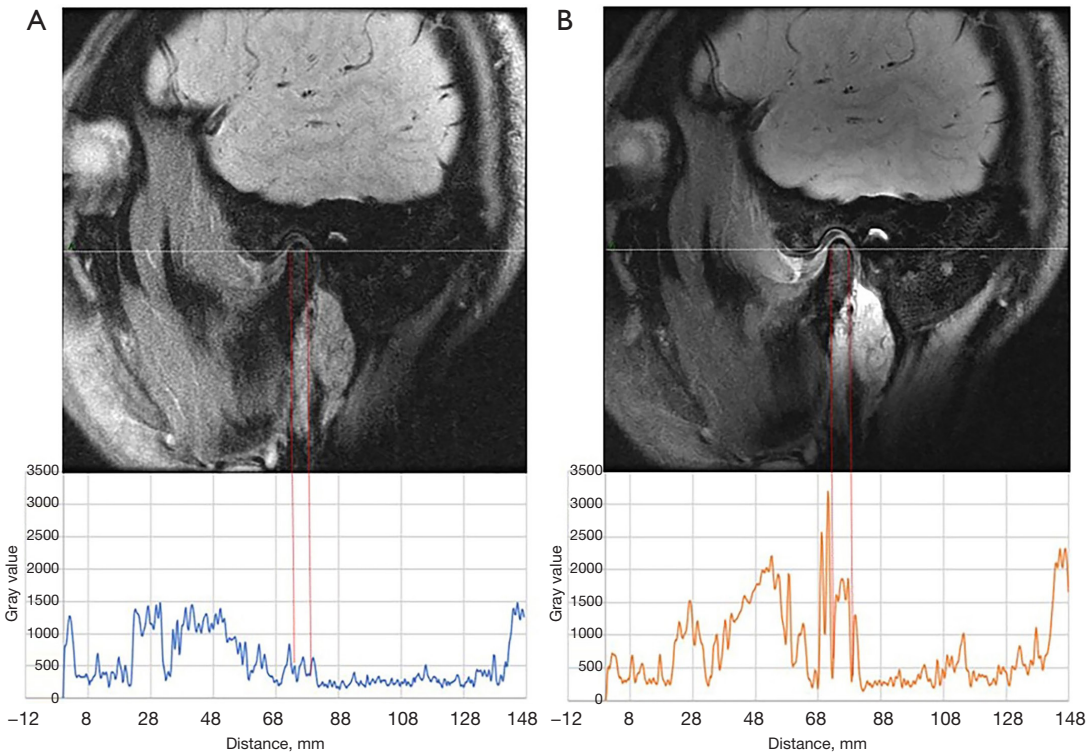

Figure 2 Difference in detection sensitivity between conventional HNCC coil and WD-HNCC. Compared to the regular image acquired by conventional HNCC coil (A), the sensitivity-enhanced image acquired by WD-HNCC (B) shows at least a 3-fold gain in detection sensitivity, clearly highlighting the condylar osseous boundaries. HNCC, head/neck coupling coiling; WD-HNCC, wireless detector–head/neck coupling coiling.

Table 1 Comparison of subjective score between the 2 groups of images ($\bar{x}$±s)

Condylar osseous changes	HNCC (mean ± SD)			WD-HNCC (mean ± SD)			Paired rank-sum test	
	Doctor 1	Doctor 1	Average	Doctor 1	Doctor 2	Average	Z	P
Osteophyte	4.00±0.60	3.92±0.51	3.96±0.50	4.92±0.29	4.83±0.39	4.88±0.23	–3.84	0.000
Cortical bone erosion	3.33±0.82	3.67±0.82	3.50±0.77	5.00±0.00	4.67±0.52	4.83±0.26	–2.80	0.005
Subcortical cyst	3.50±1.38	4.00±0.52	3.75±1.44	4.67±0.52	4.83±0.41	4.75±0.42	–3.17	0.038
Bone sclerosis	3.50±0.97	3.69±0.95	3.59±0.92	4.75±0.45	4.69±0.60	4.72±0.48	–3.71	0.000

HNCC, head/neck coupling coiling; SD, standard deviation; WD-HNCC, wireless detector-head/neck coupling coiling.

value and significance in clinical diagnosis and treatment.

With its nonradiation approach and high soft-tissue contrast, MRI has become one of the most important examination methods used for the diagnosis of TMD (17-19). However, due to the low sensitivity of conventional MRI sequences in bone cortical imaging, the use of MRI in clinical condylar bone evaluation has been limited (20,21). Increasing the field strength can improve the image quality and SNR. Some studies have confirmed that 7.0T can improve the spatial structure resolution of the TMJ articular disc (22,23). However, for the transmit radiofrequency field (RF; B1+) resulting in uneven distribution of flip angle when imaged in head at 7.0T, the flip angle in the head center is larger and the lateral region is smaller, especially the region where the TMJ is located. Hence, TMJ imaging at 7.0T has faced great challenges (22). Therefore, some

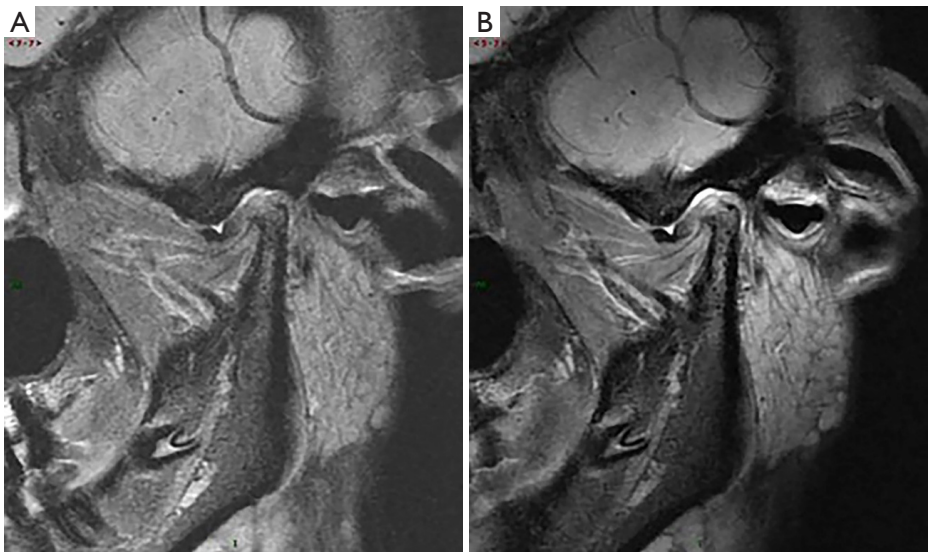

Figure 3 Display of the condylar osteophyte and erosion of the TMJ. (A) The conventional HNCC MRI image cannot show the boundary and extent of condylar osteophyte and erosion clearly enough, and subjectively, the overall image noise is higher than that of the WD-HNCC MRI image. (B) The WD-HNCC MRI image can more clearly show the boundary, extent, and morphology of osteophytes and erosion. TMJ, temporomandibular joint; HNCC, head/neck coupling coiling; MRI, magnetic resonance imaging; WD-HNCC, wireless detector–head/neck coupling coiling.

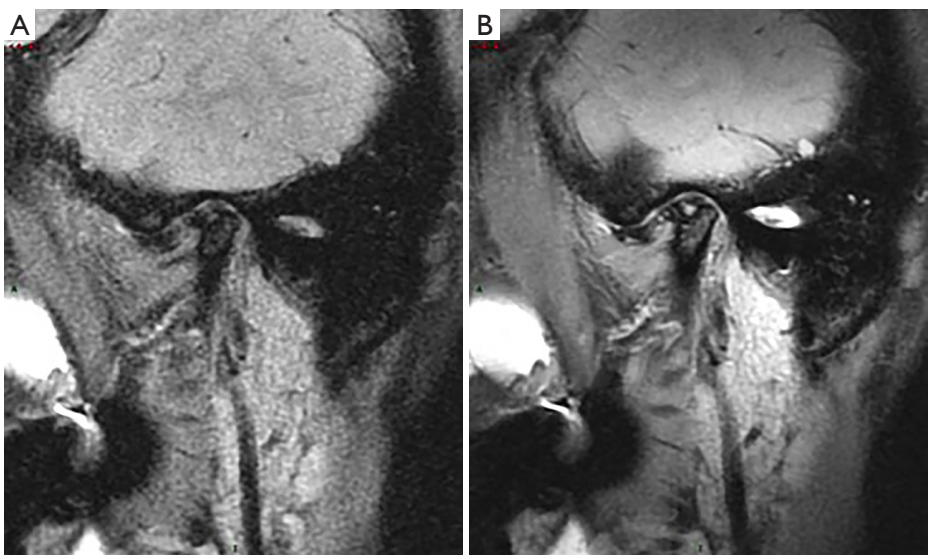

Figure 4 Images obtained by HNCC and WD-HNCC revealed extensive subcortical erosions of subcortical cysts. (A) The effect of subcortical cysts on conventional HNCC images is common. (B) The position and size of subcortical cysts are displayed more clearly on the WD-HNCC MRI scans. HNCC, head/neck coupling coiling; WD-HNCC, wireless detector–head/neck coupling coiling; MRI, magnetic resonance imaging.

additional auxiliary devices, such as dielectric pads, are needed to reduce the inhomogeneity of the field strength and improve the SNR of the TMJ (23). Moreover, 7.0T MR is not widely used in clinical application, which also limits its widespread promotion. Image enhancement can improve the accuracy of diagnosis. Montesinos *et al.* were

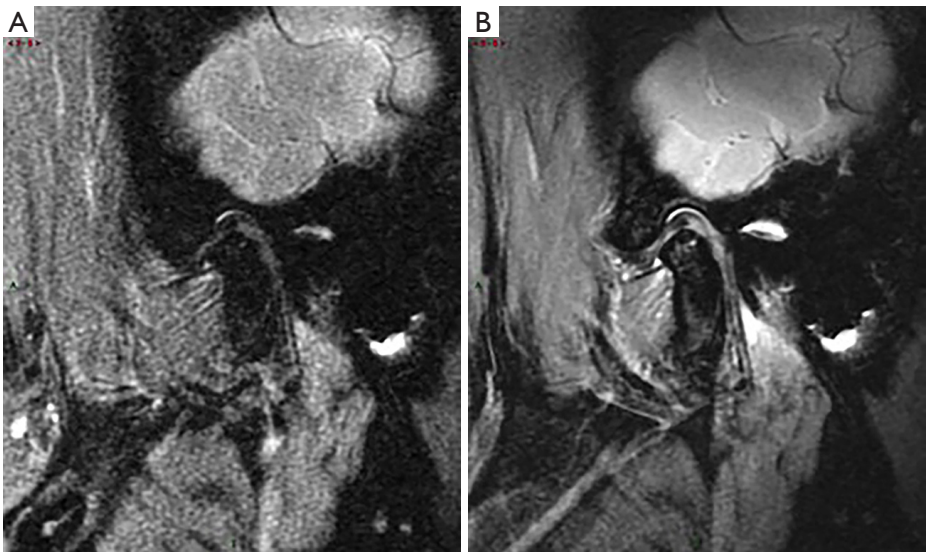

Figure 5 Display of the condylar sclerosis of the TMJ. (A) The boundary of the condylar osteosclerosis is not clear in the HNCC image. (B) The image obtained by WD-HNCC shows that the cortical part of the condylar thickens extends to the bone marrow cavity, with a clearly visible boundary. TMJ, temporomandibular joint; HNCC, head/neck coupling coiling; WD-HNCC, wireless detector–head/neck coupling coiling.

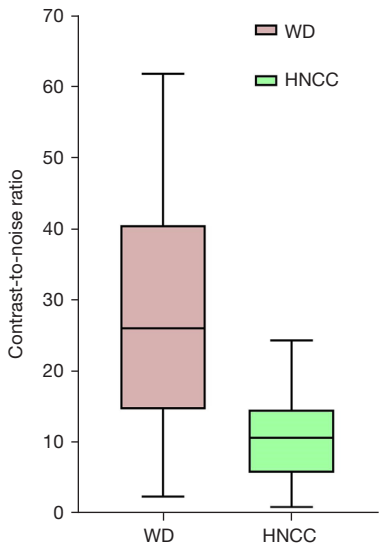

Figure 6 CNR for the WD-HNCC and HNCC MRI images. WD, wireless detector; HNCC, head/neck coupling coiling; CNR, contrast-to-noise ratio; MRI, magnetic resonance imaging.

first to apply the enhancement filters on MR images of the TMJ to investigate the subjective quality of the images and found that the images filtered with Sharpens provided better definition of the structures compared with nonfiltered images (24). However, in another study had provided the TMJ lesions, including condylar osteophytes, cystic changes, degeneration, and effusion, were shown to affect its MR manifestations (25). Recently, Lee *et al.* showed that the zero-echo time (ZTE) technique of MRI can be used to evaluate the bone changes of the TMD condyle (7). They found that the ZTE sequence showed better consistency than did CBCT in evaluating the bone changes of TMJ. Hence, MRI was expected to be a more effective method for bone evaluation of TMJ in the future. However, its clinical application is still limited by the hardware requirements and the long collection time (17).

Recent animal experiments have shown that WDs can amplify the received signal and improve detection sensitivity. A WD is a kind of local miniature signal receiving coil, which directly converts the energy collected wirelessly into an amplified MR signal via a nonlinear circuit. High-resolution scanning with WD can significantly improve tissue resolution. Compared with conventional external receivers, WD implantation can increase detection sensitivity by more than 5 times (26). A WD implanted in the corresponding position of the esophagus was found to accurately display the distal end of the common carotid artery and the vascular wall of the bifurcation of the internal and external carotid arteries after further scanning (9). Additionally, a WD used as an implantable detector mounted on the surface of the kidney was shown to improve the high-resolution imaging of renal tubules (12). This study coupled WD with conventional HNCC to performed

PDWI imaging of human TMD for the first time. The results suggested that 32 condyles clearly demonstrated different characteristics and degrees of bone changes, and the image evaluation results were highly consistent between the 2 observers. This indicated that the WD improved the visibility and capability of the conventional sequence to display condylar osseous changes. In addition, the WD-HNCC was demonstrated to obtain high-resolution and high-quality images of condyle under conventional scanning sequence (PDWI), improving the signal intensity and CNR of the condyle significantly without increasing the examination time. As a device, WD, has many advantages, such as simple appearance, easy operation, no need to connect external devices, no restriction on MR device type, and no need for special joint coils. Furthermore, the images obtained are high definition and do not need additional processing, which can meet the requirements of radiologists and stomatologists for high recognition of images, and it is thus suitable for promotion in clinical application.

This study has some limitations. First, WDs cannot be used as the gold standard at present, as the final conclusion combined the results of patients with different pathologies; a study of single-pathology imaging is needed to show the true advantage of WDs for each pathology. As we only propose use of WD as a feasible method for the noninvasive assessment of condylar bone, further in-depth clinical studies are needed for its broader application. Second, the sample size of various types of condylar osseous changes was relatively small in this study, especially in the cases with cortical erosion and cystic lesions. The authors will strive to continue to increase the sample size, laying foundations for the disease staging of condylar osseous changes in subsequent research. Finally, with the recent advanced and automatic MR imaging techniques applied to the TMJ, especially the clinical application of dynamic and quantitative MRI techniques, the scan sequence used in this study is relatively simple. In the following study, we plan to apply WDs to more advanced sequences and make use of the advantages of WDs' high resolution to explore more advantageous and accurate scan schemes in the imaging of TMJ.

Conclusions

It is feasible to use a WD for imaging of condylar osseous changes in patients with TMD, and the WD can improve the image quality of condylar bone. In the routine scanning sequence, the WD, which simultaneously images the TMJ disc and condyle with high resolution, provided the basis for a comprehensive clinical evaluation of TMD and thus possesses high potential for clinical application.

Acknowledgments

Funding: This study was supported by the National Natural Science Foundation of China (No. 82060314), the Science and Technology Foundation of Guizhou Province (No. QKHZC[2021]037), and the Guizhou Provincial People's Hospital Youth Foundation (No. GZSYQN[2019]16).

Footnote

Conflicts of Interest: All authors have completed the ICMJE uniform disclosure form (available at https://qims.amegroups.com/article/view/10.21037/qims-22-424/coif). The authors have no conflicts of interest to declare.

Ethical Statement: The authors are accountable for all aspects of the work in ensuring that questions related to the accuracy or integrity of any part of the work are appropriately investigated and resolved. The study was conducted in accordance with the Declaration of Helsinki (as revised in 2013). The study was approved by the Institutional Review Board of Guizhou Provincial People's Hospital (No. LYSZ [2019] 186), and informed consent was provided by all individual participants.

References

1. Xie C, Lin M, Yang H, Ren A. Prevalence of temporomandibular disorders and its clinical signs in Chinese students, 1979-2017: A systematic review and meta-analysis. Oral Dis 2019;25:1697-706.
2. Whyte A, Boeddinghaus R, Bartley A, Vijeyaendra R. Imaging of the temporomandibular joint. Clin Radiol 2021;76:76.e21-35.

3. Ottersen MK, Abrahamsson AK, Larheim TA, Arvidsson LZ. CBCT characteristics and interpretation challenges of temporomandibular joint osteoarthritis in a hand osteoarthritis cohort. Dentomaxillofac Radiol 2019;48:20180245.
4. Talmaceanu D, Lenghel LM, Bolog N, Hedesiu M, Buduru S, Rotar H, Baciut M, Baciut G. Imaging modalities for temporomandibular joint disorders: an update. Clujul Med 2018;91:280-7.
5. Jeon KJ, Lee C, Choi YJ, Han SS. Analysis of three-dimensional imaging findings and clinical symptoms in patients with temporomandibular joint disorders. Quant Imaging Med Surg 2021;11:1921-31.
6. Yılmaz D, Kamburoğlu K. Comparison of the effectiveness of high resolution ultrasound with MRI in patients with temporomandibular joint dısorders. Dentomaxillofac Radiol 2019;48:20180349.
7. Lee C, Jeon KJ, Han SS, Kim YH, Choi YJ, Lee A, Choi JH. CT-like MRI using the zero-TE technique for osseous changes of the TMJ. Dentomaxillofac Radiol 2020;49:20190272.
8. Zeng X, Ma S, Kruger JM, Wang R, Tan X, Qian C. High-resolution MRI of kidney microstructures at 7.05 T with an endo-colonic Wireless Amplified NMR detector. J Magn Reson 2019;303:121-7.
9. Zeng X, Barbic M, Chen L, Qian C. Sensitive enhancement of vessel wall imaging with an endoesophageal Wireless Amplified NMR Detector (WAND). Magn Reson Med 2017;78:2048-54.
10. Zeng X, Chen L, Wang C, Wang J, Qian C. Wireless MRI Colonoscopy for Sensitive Imaging of Vascular Walls. Sci Rep 2017;7:4228.
11. Zeng X, Xu S, Cao C, Wang J, Qian C. Wireless amplified NMR detector for improved visibility of image contrast in heterogeneous lesions. NMR Biomed 2018;31:e3963.
12. Zeng X, Ma S, Kruger JM, Wang R, Tan X, Qian C. High-resolution MRI of kidney microstructures at 7.05 T with an endo-colonic Wireless Amplified NMR detector. J Magn Reson 2019;303:121-7.
13. Österlund C, Berglund H, Åkerman M, Nilsson E, Petersson H, Lam J, Alstergren P. Diagnostic criteria for temporomandibular disorders: Diagnostic accuracy for general dentistry procedure without mandatory commands regarding myalgia, arthralgia and headache attributed to temporomandibular disorder. J Oral Rehabil 2018;45:497-503.
14. Alexiou K, Stamatakis H, Tsiklakis K. Evaluation of the severity of temporomandibular joint osteoarthritic changes related to age using cone beam computed tomography. Dentomaxillofac Radiol 2009;38:141-7.
15. Nickel JC, Iwasaki LR, Gonzalez YM, Gallo LM, Yao H. Mechanobehavior and Ontogenesis of the Temporomandibular Joint. J Dent Res 2018;97:1185-92.
16. Wang XD, Zhang JN, Gan YH, Zhou YH. Current understanding of pathogenesis and treatment of TMJ osteoarthritis. J Dent Res 2015;94:666-73.
17. Xiong X, Ye Z, Tang H, Wei Y, Nie L, Wei X, Liu Y, Song B. MRI of Temporomandibular Joint Disorders: Recent Advances and Future Directions. J Magn Reson Imaging 2021;54:1039-52.
18. Yılmaz D, Kamburoğlu K. Comparison of the effectiveness of high resolution ultrasound with MRI in patients with temporomandibular joint dısorders. Dentomaxillofac Radiol 2019;48:20180349.
19. Matsubara R, Yanagi Y, Oki K, Hisatomi M, Santos KC, Bamgbose BO, Fujita M, Okada S, Minagi S, Asaumi J. Assessment of MRI findings and clinical symptoms in patients with temporomandibular joint disorders. Dentomaxillofac Radiol 2018;47:20170412.
20. Alkhader M, Ohbayashi N, Tetsumura A, Nakamura S, Okochi K, Momin MA, Kurabayashi T. Diagnostic performance of magnetic resonance imaging for detecting osseous abnormalities of the temporomandibular joint and its correlation with cone beam computed tomography. Dentomaxillofac Radiol 2010;39:270-6.
21. Morales H, Cornelius R. Imaging Approach to Temporomandibular Joint Disorders. Clin Neuroradiol 2016;26:5-22.
22. Manoliu A, Spinner G, Wyss M, Ettlin DA, Nanz D, Kuhn FP, Gallo LM, Andreisek G. Magnetic Resonance Imaging of the Temporomandibular Joint at 7.0 T Using High-Permittivity Dielectric Pads: A Feasibility Study. Invest Radiol 2015;50:843-9.
23. Kuhn FP, Spinner G, Del Grande F, Wyss M, Piccirelli M, Erni S, Pfister P, Ho M, Sah BR, Filli L, Ettlin DA, Gallo LM, Andreisek G, Manoliu A. MR imaging of the temporomandibular joint: comparison between acquisitions at 7.0 T using dielectric pads and 3.0 T. Dentomaxillofac Radiol 2017;46:20160280.
24. Montesinos GA, de Castro Lopes SLP, Trivino T, Sánchez JA, Maeda FA, de Freitas CF, Costa ALF. Subjective analysis of the application of enhancement filters on magnetic resonance imaging of the temporomandibular joint. Oral Surg Oral Med Oral Pathol Oral Radiol 2019;127:552-9.
25. Bristela M, Skolka A, Eder J, Szomolanyi P, Weber M,

Piehslinger E, Schmid-Schwap M, Trattnig S. T2 mapping with 3.0 T MRI of the temporomandibular joint disc of patients with disc dislocation. Magn Reson Imaging 2019;58:125-34.
26. Qian C, Yu X, Chen DY, Dodd S, Bouraoud N, Pothayee N, Chen Y, Beeman S, Bennett K, Murphy-Boesch J, Koretsky A. Wireless amplified nuclear MR detector (WAND) for high-spatial-resolution MR imaging of internal organs: preclinical demonstration in a rodent model. Radiology 2013;268:228-36.

Cite this article as: Ming X, Cheng X, Tian C, Li W, Wang R, Qian C, Zeng X. Evaluation of condylar osseous changes using a wireless detector with proton density–weighted imaging sequences. Quant Imaging Med Surg 2023;13(1):17-26. doi: 10.21037/qims-22-424